Journal of Propulsion and Energy Vol. 1, No. 1. October 2020; 1(1): 32-43
https://doi.org/10.6108/JPNE.2020.1.1.032
pISSN 2734-1887 eISSN 2765-0049

JPNE

Numerical Simulation of Ethylene Fueled Scramjet Combustor with Air Throttling, Part 1: Auto-Ignition

Jinhyeon Noh [a] · **Jeong-Yeol Choi** [b,*] · **Vigor Yang** [c]

[a] Graduate Student, Department of Aerospace Engineering, Pusan National University, Busan 46241, Korea
[b] Professor, Department of Aerospace Engineering, Pusan National University, Busan 46241, Korea
[c] Professor, School of Aerospace Engineering, The Georgia Institute of Technology, Atlanta GA 30332, USA

Corresponding author *
Jeong-Yeol Choi
aerochoi@pusan.ac.kr

Received : 29 February 2020
Revised : 21 July 2020
Accepted : 26 July 2020

Copyright © 2020 The Korean Society of Propulsion Engineers

© This is an Open-Access article distributed under the terms of the Creative Commons Attribution Non-Commercial License (http://creativecommons.org/licenses/by-nc/3.0) which permits unrestricted non-commercial use, distribution, and reproduction in any medium, provided the original work is properly cited.

A high-resolution numerical study is carried out to investigate the auto-ignition process of ethylene fuel injection in a direct-connect scramjet combustor. Present study cares about the detailed flow evolution and flame development during the ignition transient. A quasi-global kinetics mechanism, benchmarked against detailed kinetics mechanisms, is employed to model the chemical reactions of ethylene with air in a high-speed environment. Comparing with the hydrogen fuel, the ethylene fuel is more difficult for auto-ignition, regardless of the local temperature and pressure conditions in the flame-anchoring region. The ignition delay often exceeds the flow residence time, and external means are required to achieve self-sustained combustion. As a specific example, the present research employed the air throttling to make a gas dynamic blockage downstream of the combustor. The resultant increase in the flow temperature and pressure, as well as mixing enhancement by the flow speed reduction in the pre-combustion region, greatly improves the ignition efficiency and leads to a stable flame for a while even after the air throttling is deactivated.

Key Words: Scramjet, Direct-Connect Supersonic Combustor, Ethylene, Quasi-Global Mechanisms, Air-Throttling

1. Introduction

Air-breathing hypersonic propulsion based on supersonic combustion has been studied for more than 60 years, and has proved its potential through the hydrogen-fueled Hyshot and X-43A and hydrocarbon-fueled X-51A and HyFly flight test programs [1-3]. The use of hydrocarbon fuels makes the scramjet engine much more efficient because of its higher volumetric energy density. On the other hand, hydrogen has higher energy per unit mass, higher propulsion performance, higher heat cooling capacity, and high flame speed and superior ignition characteristics. Hydrogen engines are considered as a viable propulsion system for space access, whereas hydrocarbon engines mainly considered for atmospheric flight.

One of the major obstacles in using a hydrocarbon fuel is the low flame speed (see Table 1), making it difficult to achieve complete combustion within the limited flow residence time (order of 1 ms) in a scramjet engine. The situation is further exacerbated for liquid fuels due to the time needed for atomization and evaporation. Thus, the liquid fuel is typically preheated to its supercritical state in the cooling passage. At the same time, it is cracked down to lighter species such as ethylene to have better cooling characteristics, since the process is endothermic and can absorbs additional heat [4]. Although there may exist a variety of species in cracked kerosene fuel, ethylene, C_2H_4 apparently is the dominant ingredient since its C/H ratio of 1/2 is very close to that of kerosene. Regardless of gasification of the fuel, the combustion of the hydrocarbon as scramjet fuel is still difficult due to its low flame speed, as listed in Table 1 [5].

To improve the ignition and combustion characteristics of hydrocarbon scramjet engines, several flow choking devices were employed at the end of the combustor [6]. Among them, the air throttling technique making a temporary throat aerodynamically by injecting air at the end of the combustor [7]. Thus, the combustion enhancement by the air throttling is worth of investigation by numerical means for further optimization of the hydrocarbon scramjet engine system. Present paper is further edited from the conference paper presented previously [8].

Table 1. Laminar flame speeds for various fuels in air for =1.0 and at 1 atm and room temperature [5].

Fuel	Formula	Lamina flame Speeds, SL (cm/s)
Methane	CH_4	40
Acetylene	C_2H_2	136
Ethylene	C_2H_4	67
Ethane	C_2H_6	43
Propane	C_3H_8	44
Hydrogen	H_2	210

2. Simulation Model and Numerical Approaches

2.1 Direct-Connect supersonic combustor configuration

Figure 1 shows the direct-connect supersonic flow test facility of U.S. Air Force Research Laboratory (AFRL) [9] considered for present study. It measured a length of 178.9 cm and consists of a facility nozzle, an isolator, a combustor, and an exhaust nozzle. The isolator height is 3.81 cm. The simulated flight Mach number covers the range of 3.5-6, and the dynamic pressure varies from 0.024 to 0.096 MPa. Fuel injectors are mounted on the top and bottom walls of the combustor at x=106 and 111 cm, respectively. In the present two-dimensional numerical simulations, circular injectors are replaced by two-dimensional slit of 0.11 cm width to have same exit area. The slit width is determined to have same fuel mass

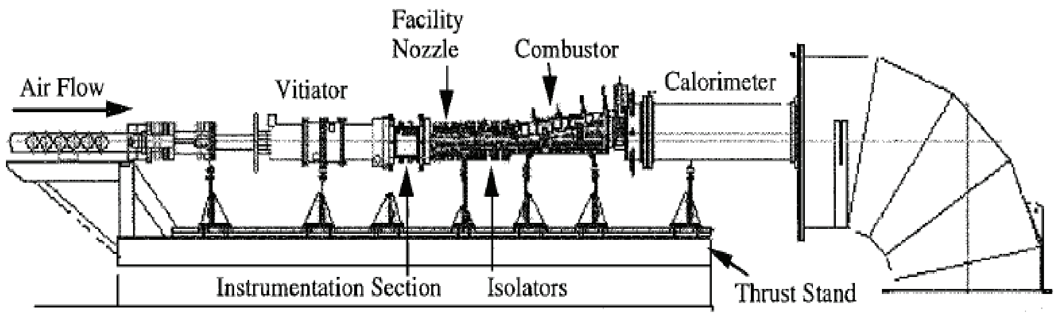

Fig. 1. AFRL direct-connect scramjet test rig [7].

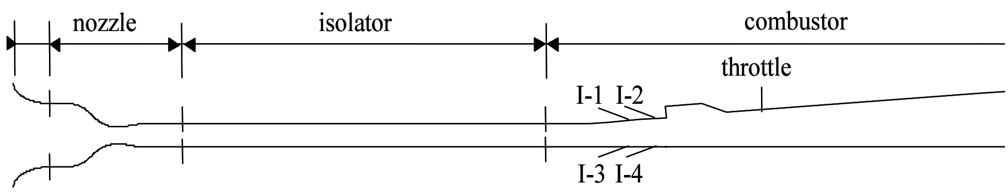

Fig. 2. Schematics of AFRL scramjet combustor [9].

flow rate. The cavity flame holder starts from 116 cm. The cavity depth is 1.7 cm, and the upper and lower lengths are 5 and 10 cm, respectively. The combustor wall diverges 2.6 degree upward, while the bottom wall remains flat. Figure 2 is the scramjet engine configuration considered in this study. Throttling air injector is also assumed as two- dimensional slit of 0.48 cm width at 136 cm along upper wall.

2.2 Computational conditions

Numerical simulations were carried out under the flight condition of Mach 5 and static pressure of 0.024 MPa. The mass flow rate of the inlet air is 0.757 kg/s, the static temperature is 1,050 K and the static pressure is 0.3744 MPa. The Mach number, static temperature and static pressure at the exit of the facility nozzle are 2.22, 560 K and 0.0328 MPa, respectively. No-lip adiabatic conditions are applied along the walls. Gaseous ethylene is injected into the combustor after the air flow is stabilized. The ethylene mass flow rate is 0.052 kg/s, corresponding to the equivalence ratio of 1.0. The ethylene fuel is injected under the Mach number 1.66, static temperature 520 K and static pressure 0.0261 MPa.

Table 2. Operation condition of the scramjet combustor.

	Static Temperature	Static Pressure	Mach No.	Injection Angles
Nozzle inlet	1,050 K	03774 MPa	0.097	
Isolator inlet	560 K	0.0328 MPa	2.22	
Fuel injection	520 K	0.0261 MPa	1.66	75 °
Air throttle	273 K	0.1920 MPa	1.00	90 °

Air throttle is mounted at the top of the combustor wall at x=136 cm which injects 0.151 kg/s air vertically downward at sonic speed, 1 ms after the fuel injection with static temperature 273 K and static pressure 0.1920 MPa. All the flow conditions are summarized in Table 2.

2.3 Two-Dimensional simulation

The AFLR scramjet combustor considered in this has rectangular cross-section. Therefore, two-dimensional modeling could be considered as a reasonable first step of modeling. However three-dimensional effect should be cared about for several reasons. The one is the aerodynamics effect. Due to the presence of the side wall, the effective cross section area of flow passage is reduced than the two-dimensional model by the presence of wall boundary layer along the side walls. The corner flow effect may reduce further the effective cross-section area. The reduction of effective cross section area results in the pressure rise downstream. It is also found that the boundary layers at upper and lower walls are connected through the boundary layer at side wall which would be important for flame propagation during ignition transients [7]. The three-dimensional effect is especially important for the combustion since the diffusive supersonic combustion is governed by the fuel/air mixing that is linearly dependent on the contact area. Three-dimensional eddy is considered to have about the twice of the surface area than that of two-dimensional eddy from the analogy of the surface areas of cylinder and sphere [10]. Therefore three- dimensional effects further enhance the combustion and two-dimensional simulation would under-predict the combustion and

 Copyright © 2020 The Korean Society of Propulsion Engineers

propulsion efficiency. Modeling of three-dimensional hole injection to two-dimensional slit injection results in the same consequence.

Regardless of these limitations, two-dimensional simulation still has great advantages coming from the efficiency. Considering order of 100 grid points in span-wise direction, efficiency of two-dimensional simulation is 1/100 of three-dimensional simulation while maintaining same resolution. Therefore, the LES (large eddy simulation) level fine resolution simulation is possible for full scale supersonic combustor for the sufficiently long time of operation including the ignition transients, for which full 3D LES simulation is not much successful until now. Also, the computational efficiency gives more chances of parametric studies. Another benefit of the efficiency is that the relatively small data size makes further post-processing and data mining possible, those are crucial to understand the underlying physics. Thus, it is considered that the two-dimensional simulation is still useful for the qualitative understanding of the unsteady operation characteristics while resolving turbulence eddy motions though it may under-predict the combustion performance.

2.4 Physical models and numerical approaches

The flowfield is assumed to be two-dimensional for computational efficiency that can be described with the conservation equations for a multi-component chemically reactive system. The coupled form of the species conservation, fluid dynamics, and turbulent transport equations can be summarized in a conservative vector form as follows.

$$\frac{\partial \mathbf{Q}}{\partial t}+\frac{\partial \mathbf{E}}{\partial x}+\frac{\partial \mathbf{F}}{\partial y}=\frac{\partial \mathbf{E_v}}{\partial x}+\frac{\partial \mathbf{F_v}}{\partial y}+\mathbf{W} \qquad (1)$$

where,

$$\mathbf{Q}=\begin{bmatrix}\rho_j\\ \rho u\\ \rho v\\ \rho e\\ \rho k\\ \rho\omega\end{bmatrix},\quad \mathbf{E}=\begin{bmatrix}\rho_j u\\ \rho u^2+p\\ \rho uv\\ (e+p)u\\ \rho uk\\ \rho u\omega\end{bmatrix},\quad \mathbf{F}=\begin{bmatrix}\rho_j v\\ \rho uv\\ \rho v^2+p\\ (e+p)v\\ \rho vk\\ \rho v\omega\end{bmatrix},$$

$$\mathbf{W}=\begin{bmatrix}\omega_j\\ 0\\ 0\\ 0\\ S_k\\ S_\omega\end{bmatrix},\quad \mathbf{E_v}=\begin{bmatrix}-\rho_j u_j^d\\ \tau_{xx}\\ \tau_{xy}\\ \beta_x\\ \mu_k\partial k/\partial x\\ \mu_k\partial\omega/\partial x\end{bmatrix},\quad \mathbf{F_v}=\begin{bmatrix}-\rho_j u_j^d\\ \tau_{yx}\\ \tau_{yy}\\ \beta_y\\ \mu_k\partial k/\partial y\\ \mu_k\partial\omega/\partial y\end{bmatrix} \qquad (2)$$

The subscript *k* denotes reaction species (O, O_2, H, H_2, OH, H_2O, CO, CO_2, C_2H_4) from 1 to N. Nitrogen is regarded as inert gas since it has little effects on chemical kinetics and heat of reaction. The vector **Q** is the conservative variable vector and the vector **W** is the source term vector. Convective flux vector **E** and **F** are discretized by the Roe's flux difference splitting (FDS) method and viscous flux vector **Fv** and **Gv** are discretized by a central difference method. The computational code has been used before for a supersonic combustor study [11] and currently extended to fifth order accurate scheme [12]. The Menter's shear stress transport (SST) model is used with SST DES (detached eddy simulation) extension [13] to enhance the eddy capturing characteristics at separated flow region while preserving the RANS characteristics at boundary layer. The second order implicit time integration is used with sub-iterations for time accurate computation. The two-dimensional code is parallelized by OpenMP for the optimum performance in multi-core SMP (shared memory processors) machines.

Hydrogen combustion mechanism is taken from GRI-Mech 3.0 used in the previous study [11]. For the ethylene reaction mechanism Singh and Jachimowski's quasi-global chemistry mechanism, as listed in Table 3, involving 10 elementary reaction steps and 8 reaction species is used [14]. Though there are more recent studies on reduced combustion mechanism of ethylene for supersonic combustion [15,16], none of them are available in public domain and Singh and Jachimowski's mechanism is one of the simple mechanism available. Also, it could better predict the equilibrium condition than the global chemistry model by considering the intermediate species.

For the validation of the reliability of the mechanism, the auto ignition profile at given pressure and temperature is compared in Fig. 3 with that of USC Mech-II, a detailed mechanism for gaseous hydrocarbon fuels [17]. Pre-exponential facto and activation energy of fuel decomposition reaction (Reaction No. 1 in Table 3) is tuned to have better agreement with the detailed chemistry. It is shown that the quasi-global mechanism shows smoother profile time than the detailed model that would be better for numerical stability. Ignition delay time is summarized in

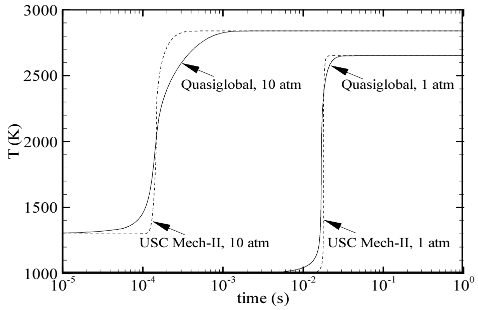

Fig. 3. Comparison of constant pressure ignition profiles by quasi-global mechanism [14] and USC-Mech II [17].

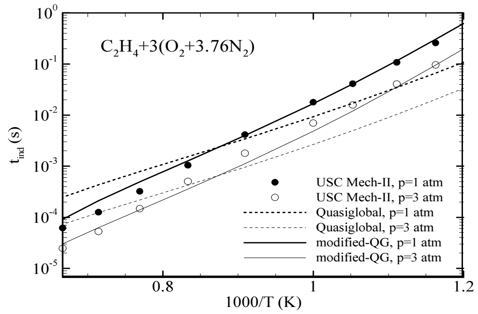

Fig. 4. Comparison of constant pressure ignition delays by quasi-global mechanism [14] and USC-Mech II [17].

Table 3. C_2H_4 - O_2 reaction system[a] (10 step).

No.	Reaction	A	n	E
1	$C_2H_4 + O_2 \Leftrightarrow 2CO + 2H_2$	1.80E14 [c]2.00E16	0.0	35,500 [c]47,000
2[b]	$CO + O \Leftrightarrow CO_2 + M$	5.30E13	0.0	-4540
3	$CO + OH \Leftrightarrow CO_2 + H$	4.40E06	1.5	-740
4	$H_2 + O_2 \Leftrightarrow OH + OH$	1.70E13	0.0	48,000
5	$H + O_2 \Leftrightarrow OH + O$	2.60E14	0.0	16,800
6	$OH + H_2 \Leftrightarrow H_2O + H$	2.20E13	0.0	5,150
7	$O + H_2 \Leftrightarrow OH + H$	1.80E10	1.0	8,900
8	$OH + OH \Leftrightarrow H_2O + O$	6.30E13	0.0	1,090
9[b]	$H + H \Leftrightarrow H_2 + M$	6.40E17	-1.0	0
10[b]	$H + OH \Leftrightarrow H_2O + M$	2.20E22	-2.0	0

[a]Units are in seconds, moles, cubic centimeters, calories, and degrees Kelvin,
[b]Third-body efficiencies for all termolecular reactions are 2.5 for M = H2, 16.0 for H2O, and 1.0 for all other M.
[c]Modified for better prediction in the present study

Copyright © 2020 The Korean Society of Propulsion Engineers

Fig. 4 within the operation range considered. The quasi-global mechanism has shorter ignition delay for the temperatures lower than about 1,100 K at 1 atm and 1,200 at 10 atm. It is found that the quasi-global mechanism is not fully agrees with the detailed mechanism but has acceptable agreement with the detailed mechanism considering the reaction zone profile and the ignition delay time.

2.5 Grid refinement study

The computational grid must be fine enough to trust the simulation results, while the grid numbers should be minimized the computation resource and cost. To make decision by a trade-off the, a grid refinement study is conducted. The grid numbers are tabulated in Table 4 along the grid levels. Five grids systems are adopted to validate two-dimensional code and define the most effective and accurate grid model. At first, dependency on longitudinal grid resolution is tested while maintaining the number of vertical grid points for combustor and cavity are fixed at 101 and 81. As a next step, dependency on vertical grid resolution is tested while maintaining the number of longitudinal grid points is fixed at 1,205. After stabilizing the cold air flow the upper wall pressure data of the two-dimensional simulation are compare with the experimental data and 3-dimensional data of Li et al. [7] and they are depicted in Fig. 5 and 6 for each test respectively. All the grid resolutions show the agreement at isolator section due to the boundary layer growth. It is clear that two- dimensional results under- predict the pressure distribution by the neglecting the side-wall effects. The two-dimensional results show about 30% error around the injector and cavity region. However, general trends of pressure variation are similar to three-dimensional or experimental data. In longitudinal grid resolution test, grid level 1, 2, 3 have less than 3% relative errors. However, the level 1 grid is not able to detect shock train inside the isolator correctly and grid level 3 consumes much computation resource. Thus, the 1,205 grids are selected for the longitudinal grid number. Vertical grid resolution test shows that the grid level 4 underestimates the pressure inside the combustor more than the grid level 2 and 5 generally. The relative error of grid level 2 and 5 are around 1%, and the 101 grids are selected for the vertical direction.

Table 4. Grid systems for the convergence test.

Grid	Scramjet	Cavity	Total number of grid points
L1	603×101	75×81	66,903
L2	1205×101	150×81	133,855
L3	2415×101	300×81	268,215
L4	1205×81	150×81	109,755
L5	1205×121	150×81	157,955

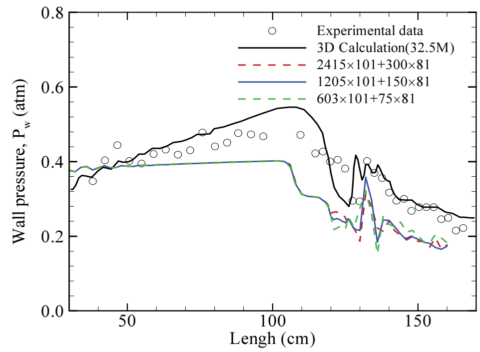

Fig. 5. Comparison of wall pressure depending on longitudinal grid resolutions for non-reacting case.

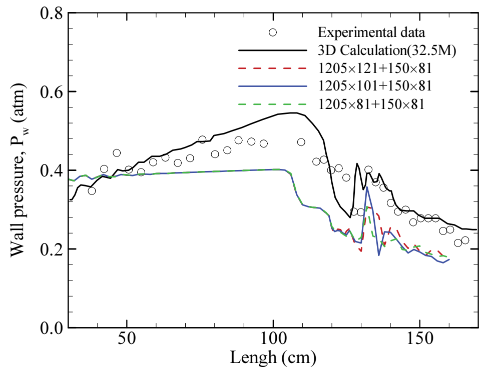

Fig. 6. Comparison of wall pressure depending on vertical grid resolutions for non-reacting case.

3. Results and Discussion

3.1 Comparison of hydrogen and ethylene injection without air throttling

To compare the general characteristics of hydrogen and ethylene injection and combustion in supersonic air stream, numerical simulations are carried out for hydrogen and ethylene with same equivalence ratio of 1.0 and same injection scheme. Fig. 7 is the resulting instantaneous temperature contour and pressure distributions overlaid with iso-Mach number line of 1.0 at the end of each computation. For hydrogen, fuel mixes very well and self-ignites by the increase of temperature caused by air stagnation from the interaction of fuel and air, though the inflow temperature is little bit low for self-ignition. Higher diffusion of hydrogen could have a role in the mixing of hydrogen and air. Combustion of hydrogen increases the back pressure and the combustion is enhanced further. Shock train is formed in the middle of the isolator maintaining the pressure build up to the combustor. It is found from the iso-Mach line that the flow is not choked, and the supersonic combustion is established. Fig. 8 is the pressure history at x=118 cm inside the cavity. Pressure increase by the combustion is shown 1 ms after the hydrogen injection. Therefore, it is considered that the necessary time for the establishment of hydrogen combustion by auto ignition is the order of flow characteristic time of the supersonic combustor. After the combustion establishment, stable combustion is maintained though there is gradual increase in pressure caused by the gradual increase of the combustion efficiency.

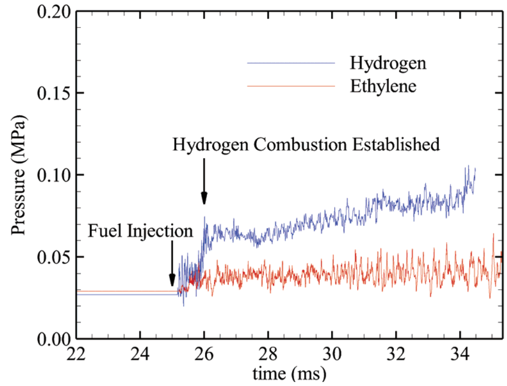

Fig. 8. Pressure histories at x=118 cm for hydrogen and ethylene injection cases without air throttle.

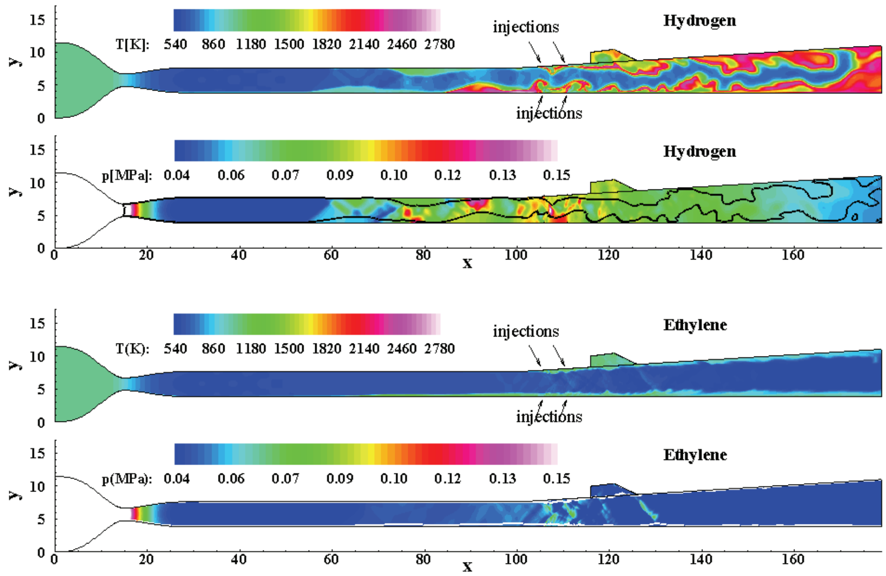

Fig. 7. Temperature and pressure distributions for hydrogen and ethylene injection cases without air throttle.

Copyright © 2020 The Korean Society of Propulsion Engineers

In case of ethylene injection, it is shown that the fuel neither ignites nor mixes with air. It is partly because the low diffusion of ethylene, but mainly by lower flame speed or longer ignition delay than that of hydrogen. The fuel injection makes the flow becomes unstable and turbulent fuel stream along the walls while generating weak shock train around the middle of the combustor. The temperature inside the cavity increases around 1,000 K due to flow stagnation, but the fuel residence time is considered not enough for the self-ignition. Since the two-dimensional simulation may under-predicts the pressure and temperature, there is better possibility of combustion for three-dimensional simulation. The pressure variation by the ethylene injection is also shown in Fig. 8, but only shows turbulent fluctuation caused by fuel injection without further increase.

3.2 The starting process with air throttling

To ignite ethylene fuel, air throttle is imposed at the expansion part of the combustor 1 ms after fuel injection. The throttling air is injected as a step function for the simplicity, although the sudden increase in injection pressure would be not available in practice, and the flow development would strongly depend on pressure increase rate. The air throttle is maintained for 12 ms and is turned off later. The time sequence of the ignition process is plotted by the series of the temperature contours in Fig. 9, pressure contours in Fig. 10, pressure gradient plot in Fig. 11 and CO_2 distribution in Fig. 12. Different variables are plotted in these figures for better understanding of combustion characteristics by comparison.

At t=25.1 ms, 0.1 ms after fuel injection, shock train begins to form around the injector. At t=26.1 ms, 0.1 ms after air throttle on, bow shock appears ahead of the throttling air resulting pressure build up ahead. At t=27.6 ms, 1.6 ms after air throttling, temperature and pressure have been build up to about 1,000 K and 1 atm, but the combustion is not fully established yet. Shock train is formed ahead of injectors through the non-reacting air flow in the isolator. The combustion is finally established about 4 ms after air throttling, as shown at t=30.1 ms. During this period, shock train is fully formed ahead of the combustion region inside the isolator. However

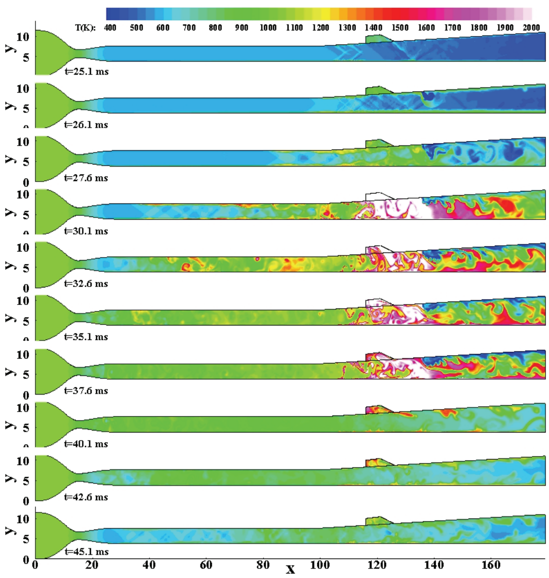

Fig. 9. Transients of temperature distributions with air throttle.

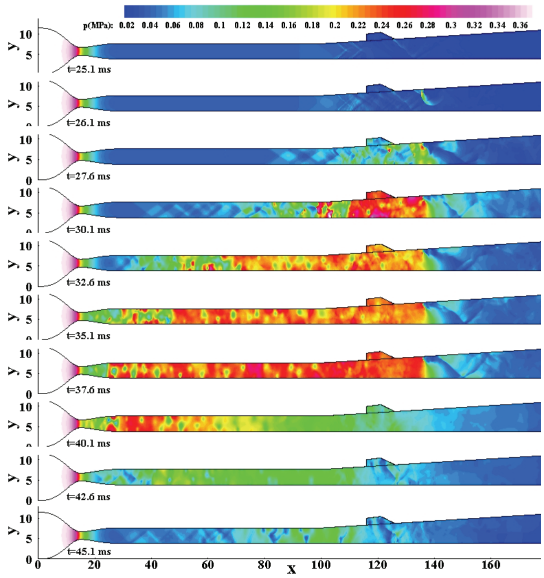

Fig. 10. Transients of pressure distributions with air throttle.

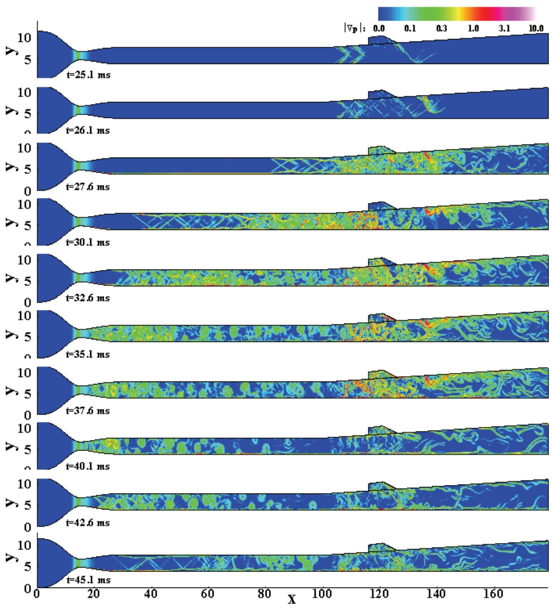

Fig. 11. Transients of pressure gradient plots with air throttle.

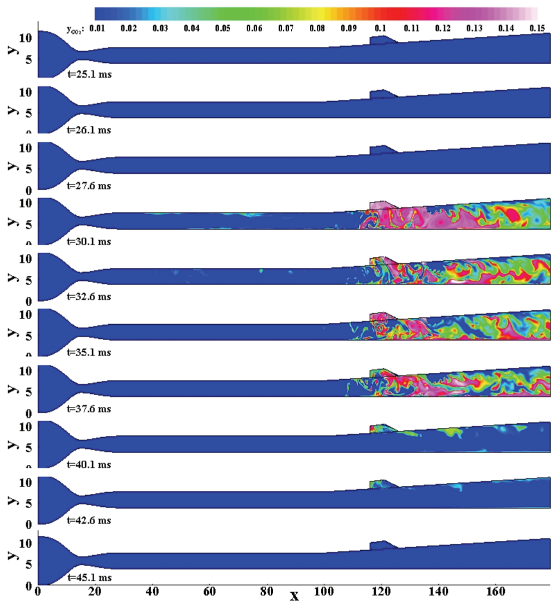

Fig. 12. Transients of CO_2 mass fraction distributions with air throttle.

secondary shock train is overlapped and moving forward due to the thermal choking effect at the combustion region. Since the equivalence ratio of 1.0 is quite a strong condition for scramjet mode operation, pressure is built up continuously ahead of the injector and the shock train finally reaches close to the inlet nozzle throat at t=37.6 ms. At this period, fuel is burned out near completely, resulting maximum amount of heat addition within the combustor. This result corresponds to the unstart of the scramjet engine by choking. Reminding that 1 ms after fuel injection is sufficient for combustion establishment for hydrogen case, it is understood that the ethylene fuel needs relatively long ignition delay (order of 3 ms), even with the flow speed reduction by blockage effect from the air throttling. The slow kinetics of ethylene is considered as major reason for the long ignition delay, since the effects of molecular diffusion or turbulent mixing would have been increased significantly by the blockage effect.

After the air throttling is turned off at 37.6 ms, the combustion gas expands freely at supersonic speed

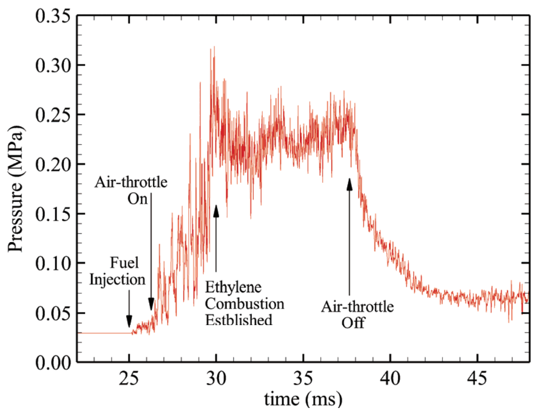

Fig. 13. Pressure histories at x=118 cm for ethylene injection case with air throttle.

without blockage. Following the air throttling turned off the isolator and the combustor is depressurized continuously the oblique shock train is recovered. According to the depressurization of the combustor, the combustion fades off though the flame is stabilized for a long time within the cavity. The pressure history at x=118 cm inside the cavity in Fig. 13 shows better perspective on the progress.

Copyright © 2020 The Korean Society of Propulsion Engineers

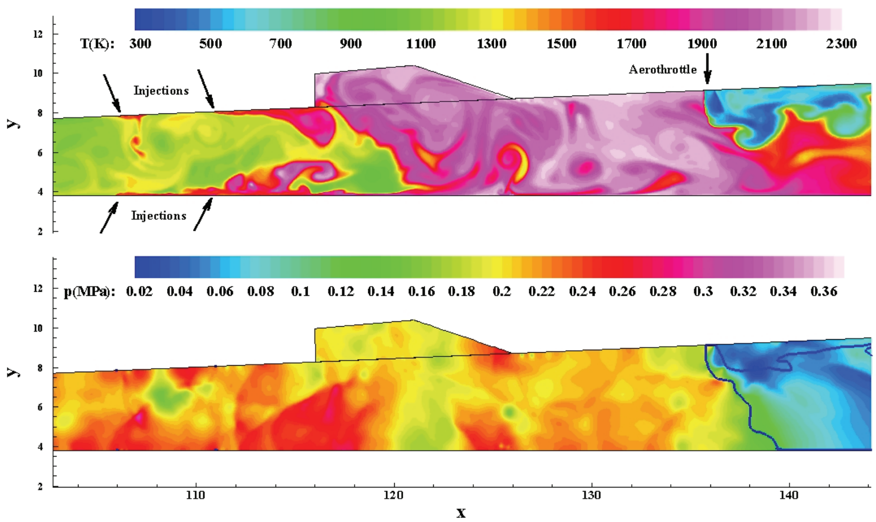

Fig. 14. Temperature pressure distributions at t=30 ms.

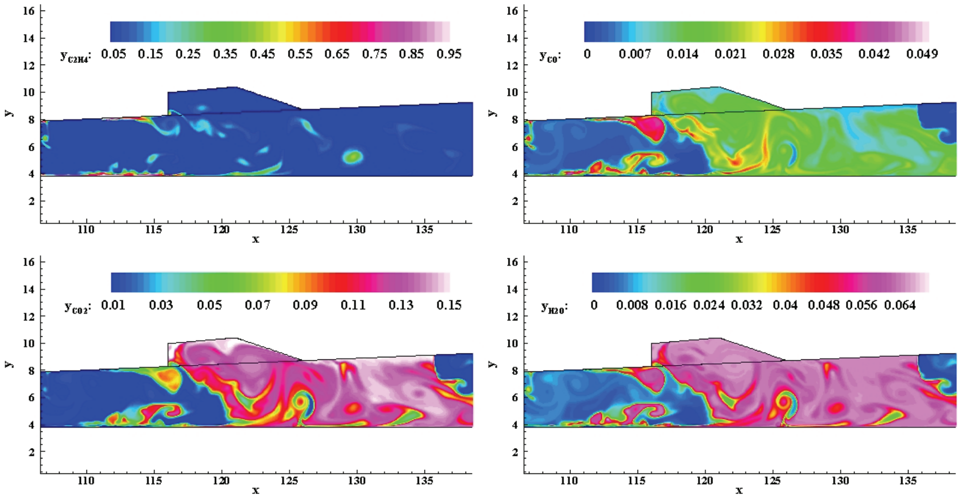

Fig. 15. Fuel and product mass fraction distributions at t=30 ms.

It is understood that about 4 ms of delay was required for combustion establishment caused by the slow mixing of ethylene and air mixing and longer ignition delay. Pressure is not stabilized after the combustion establishment due to the transient processed within the combustor and isolator. After the air throttling off, the pressure decreases gradually to 0.7 MPa level, though the stationary combustion is not fully attained.

Figure 14 and 15 gives more insight into the combustion and hydrodynamic process that combustion of fuel and production of burned gas is controlled by the turbulent flow motions. It is clearly found that air throttling jet acts as a gas-dynamic throat which makes pressure build-up ahead and burned gas expands to supersonic flows downstream. It is also found that the air throttling jet itself is unstably fluctating as shown in the rear part of temperature contour in Fig. 14. This flow patter is considered as Kelvin-Helmholtz instability, which finally has turbulent flow characteristic.

4. Conclusion

Numerical studies on the transient process of ethylene fuel injection and air throttling process gives further insight into the ignition characteristics and combustion dynamics of ethylene combustion in supersonic air stream. Comparison of the hydrogen and ethylene injection showed that the ethylene is much more difficult to ignite and gives the justification of the additional ignition device such as air throttling. The application of air throttle shows detailed transient flow features in the scramjet combustor giving further insight of into the combustion dynamics in scramjet engine operation, regardless of many limitations from two-dimensional modeling, turbulence, and chemical kinetics. Due to the slower kinetics than hydrogen, that about 4 ms of delay is necessary prior to establishment of ethylene combustion, that is quite a long time in comparison with the flow characteristic time scramjet combustor.

Acknowledgements

Present paper is sponsored for publication by the Basic Research Program (No. 08-201-501-014) of the Agency for Defense Development (ADD) supported by the Defense Acquisition Program Administration (DAPA) of the Korean Government.

References

1. Peebles, C., Road to Mach 10: lessons learned from the X-43A flight research program, Library of Flight Series, American Institute of Aeronautics and Astronautics, Reston, 2008.
2. Hank, J.M, Murhy, J.S. and Mutzman, R.C., “The X-51A Scramjet Engine Flight Demonstration Program,” AIAA 2008-2540, 15th AIAA International Space Planes and Hypersonic Systems and Technologies Conference, Dayton, Ohio, April 28-May 1, 2008.
3. Noh, J., Won, S.-H., Parent, B., Choi, J.-Y., Byun, J.-R., and Lim, J.-S., “Core Technologies of the X-51A SED-WR Program,” Journal of the Korean Society of Propulsion Engineers, Vol. 12, No. 5, Oct. 2008, pp.79-91.
4. Edwards, T., “Liquid Fuels and Propellants for Aerospace Propulsion: 1903–2003,” Journal of Propulsion and Power, Vol.19. No.6, 2003, pp.1089-1107.
5. Law, C.K., “Compilation of Experimental Dataon Laminar Burning Velocities,” in Reduced Kinetic Mechanisms for applications in Combustion Systems (N. Peters and B. Rogg, eds.), Springer-Verlag, New York, p.15-26, 1993.
6. Donbar, J., Powell, O., Gruber, M., Jackson, T., Eklund, D. and Mathur, T., “Post-test Analysis of Flush-Wall Fuel Injection Experiments in a Scramjet Combustor,” AIAA Paper 2001-3197.
7. Li, J., Zhang L., Choi, J.-Y., Yang, V. and K.-C. Lin, "Ignition Transients in an Ethylene Fueled Scramjet Engine with Air Throttling Part I: Non-Reacting Flow," Journal of Propulsion and Power, Vol.30, No.2, Mar.-Apr. 2014, pp. 438-448. http://dx.doi.org/10.2514/1.B34763
8. Noh, J.-H., Choi, J.-Y., Byun, J.-R., Gil, H.-Y. and Lim, J.-S., “Numerical Study of the Auto-Ignition by Aero-throttling in an Ethylene Fueled Scramjet Engine,” AIAA 2010-7036, 46th AIAA/ASME/SAE/ASEE Joint Propulsion Conference & Exhibit, Jul. 25-28, 2010, Nashville, TN.
9. Gruber, M., Donbar, J., Jackson, K., Mathur, T., Baurle, R., Eklund, D. and Smith, C., “Newly Developed Direct-Connect High-Enthalpy Supersonic Com- bustion research Facility,” Journal of Propulsion and Power, Vol. 17, No. 6, pp. 1296-1304.

Copyright © 2020 The Korean Society of Propulsion Engineers

10. Hinterberger, C., J. Fröhlich, and W. Rodi. “Three-dimensional and depth-averaged large-eddy simulations of some shallow water flows,” Journal of Hydraulic Engineering, Vol.133 No.8, 2007, pp. 857-872.
11. Choi, J.-Y., Yang, V. and Ma., F., "Combustion Oscillations in a Scramjet Engine Combustor with Transverse Fuel Injection,” Proceedings of the Combustion Institute, Vol. 30/2, Jan. 2005, pp. 2851-2858.
12. Shin, J.-R., Moon, S.-H., Won, S.-H., and Choi, J.-Y., “Detached Eddy Simulation of Base Flow in Supersonic Mainstream,” Journal of KSAS, Vol.37, No.10, Oct. 2009, pp.955~966.
13. Strelets, M., “Detached Eddy Simulation of Massively Separated Flows,” AIAA Paper 2001-0879, 2001.
14. Singh, D.J. and Jachimowski, C.J., “Quasigolbal Reaction Model for Ethylene Combustion,” AIAA Journal, Vol. 32, No.1, pp213-216.
15. Liu, J., Tam, C., Lu, T. and Law, C.K., “Simulations of Cavity-stabilized Flames in Supersonic Flows Using Reduced Chemical Kinetic Mechanisms,” AIAA 2006-4862.
16. Hitch, B.D., Lynch, E.D., “Use of Reduced, Accurate Ethylene Combustion Mechanisms for a Hydrocarbon-Fueled Ramjet Simulation”, AIAA 2009-5384, 45th AIAA/ASME /SAE/ASEE Joint Propulsion Conference & Exhibit, August 2-5, 2009, Denver, Colorado.
17. Wang, H., You, X., Joshi, A.V., Davis, S.G., Laskin, A., Egolfopoulos, F. and Law, C.K., USC Mech Version II. High-Temperature Combustion Reaction Model of H2/CO/C1-C4 Compounds. http://ignis.usc.edu/USC_Mech_II.htm, May 2007.